JOURNAL OF MATERIALS SCIENCE 25 (1990) 3901–3905

Diametral compression tests of silicon carbide fibre-reinforced glass

AKIRA OKADA
Central Engineering Laboratories, Nissan Motor Co., Ltd, Yokosuka, Kanagawa 237, Japan

Diametral compression tests were carried out for unidirectionally aligned silicon carbide fibre-reinforced borosilicate glass. The fracture load dependence on the angle between the loading axis and the fibre alignment was investigated. The stress components in the fibre-aligned plane were calculated to evaluate the effect of the shear stress on fracture. Weibull statistics were employed to estimate the fracture load dependence on the fibre orientation angle. Assuming $m = 5$ to 10, the contribution of shear stress to the fracture of silicon carbide fibre-reinforced glass was found to be negligible.

1. Introduction

Fracture of brittle materials is believed to occur when the stress intensity factor for the worst pre-existing crack reaches the critical value. This critical value coincides with mode I fracture toughness, K_{IC}, when the normal tensile stress is applied to the crack. The critical value for a crack exposed to the complex loading of tension and shear should, however, be given by the mixed-mode fracture criterion.

Although several expressions have been proposed for the mixed-mode fracture from theoretical viewpoints [1–4], it has been difficult to determine an adequate expression for experimental adaptation. This is partially owing to the experimental difficulty in finding the mixed-mode fracture criterion, which is determined not only from the stress initiating the crack propagation, but also from the angle between the main crack and the direction of the crack extension. Furthermore, crack extension under mixed-mode loading tends to change the angle for reducing the shear components of the crack [1, 5, 6], whereas the angle at initiation is strongly affected by the microstructure and the cleavage characteristics of the material.

Unidirectionally fibre-reinforced materials have the capability to control crack extension during complex loading because the crack tends to propagate along the fibre axis. This is also an advantage when investigating the mixed-mode fracture criterion because it makes simplified expression possible. The objective of the present study was thus to explore the mixed-mode fracture criterion in diametral compression tests on fibre-reinforced glass.

2. Experimental procedure

The disc specimens used in this study were made of silicon carbide fibre-reinforced borosilicate glass produced by Nippon Carbon Co., Japan. The silicon carbide fibres were Nicalon, also made by Nippon Carbon Co., and unidirectionally aligned along the disc plane having a fibre volume fraction of 50%. The composite had a density of 2.3 g cm^{-3}, and the dimensions of the disc specimen were 20 mm diameter and 5 mm thick. The diametral compression tests were carried out using a universal testing machine having a crosshead speed of 0.5 mm min^{-1}. Writing paper was inserted between the compression plate and the disc specimen to prevent the specimen from rolling. In order to measure the angle between the fibre alignment and the loading axis, photographs of the specimen were taken after fracture occurred accompanied by a sudden load drop.

3. Results and discussion

Fig. 1 shows the results of fracture load during the diametral compression tests against the angle between the loading axis and the fibre alignment. For an angle smaller than 30°, the fracture load increases with increase in the angle. Specifically, the fracture load, which is approximately 4000 N at 5°, increases to 6000 N at 30°. In this case, the cracks are introduced into the disc plane along the fibre axis. For angles greater than 30°, the crack propagates along the side plane of the disc. The fracture load is an approximately constant value of 6000 N though considerable scattering is observed.

Typical cracks produced in the disc specimens are shown in Fig. 2. Vertical cracking along the fibre plane is observed when the loading axis is approximately parallel to the fibre axis (Fig. 2a). Fracture at an angle of 10° is shown in Fig. 2b. Here, the crack arrested in the middle of the disc seems to have been initiated from the lower loading point of the disc. Crack propagation at an angle of 25° is shown in Fig. 2c. In this case, the crack starts from the upper loading point and extends to the opposite side of the specimen along the fibre plane, resulting in fracture with sliding of the cracked plane. Finally, fracture at an angle of 85° is shown in Fig. 2d. Vertical cracking is observed in the side of the disc with no cracks being produced in the disc plane.

Because the diametral compression strength shows

0022–2461/90 $03.00 + .12

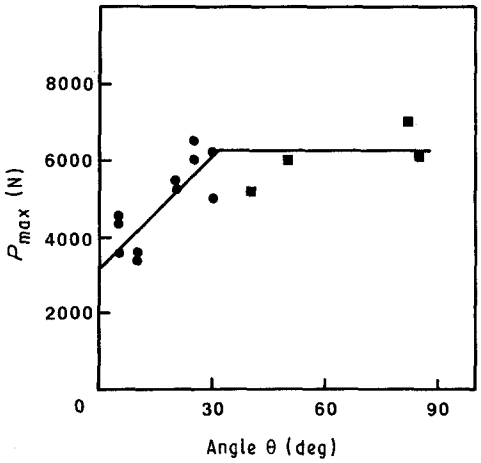

Figure 1 Fracture load in diametral compression tests of silicon carbide fibre-reinforced borosilicate glass plotted against the angle between the loading axis and the fibre alignment. (●) Fracture in the disc plane, (■) fracture along the side of the disc.

no dependence on the fibre orientation at angles greater than 30°, it is concluded that the tensile stress in the thickness direction governs the fracture. On the other hand, the fracture load dependence on an angle smaller than 30° suggests that the stress state in the inclined plane along the fibre governs the fracture.

At the loading points of the fractured specimen, crushed zones caused by the compression were observed in the range of almost one-tenth of the disc diameter. Thus, it is assumed that the stress distribution can be given by the elastic theory incorporating a minor correction.

Fig. 3 shows the configuration of the disc specimen under diametral compression. The elastic stress components are given by [7]

$$\sigma_x = -2P/\pi t\left[(R-y)x^2/r_1^4 + (R+y)x^2/r_2^4 - \frac{1}{2R}\right] \quad (1a)$$

$$\sigma_y = -2P/\pi t\left[(R-y)^3/r_1^4 + (R+y)^3/r_2^4 - \frac{1}{2R}\right] \quad (1b)$$

and

$$\tau_{xy} = 2P/\pi t\,[(R-y)^2 x/r_1^4 - (R+y)^2 x/r_2^4] \quad (1c)$$

where $r_1 = [x^2 + (R-y)^2]^{1/2}$, $r_2 = [x^2 + (R+y)^2]^{1/2}$, P is load, R is the disc radius, and t is the disc thickness. The normal stress, σ_n, and the shear stress, τ, in the inclined plane having an angle θ are given by [8]

$$\sigma_n = \sigma_x \cos^2\theta + \sigma_y \sin^2\theta + \tau_{xy} \sin 2\theta \quad (2a)$$

and

$$\tau = [-(\sigma_x - \sigma_y)/2] \sin 2\theta + \tau_{xy} \cos 2\theta \quad (2b)$$

The normal and shear stress components in the arbitrary plane can be calculated by substituting Equation 1 into Equation 2.

Fig. 4 indicates the tensile and compressive stress regions of the normal stress in the inclined plane. When the inclined angle is 0°, the normal stress through the loading axis is tensile and the compression region does not appear on this axis of the disc. Inclining the angle, however, leads to expansion of the compressive stress region in the inclined plane passing

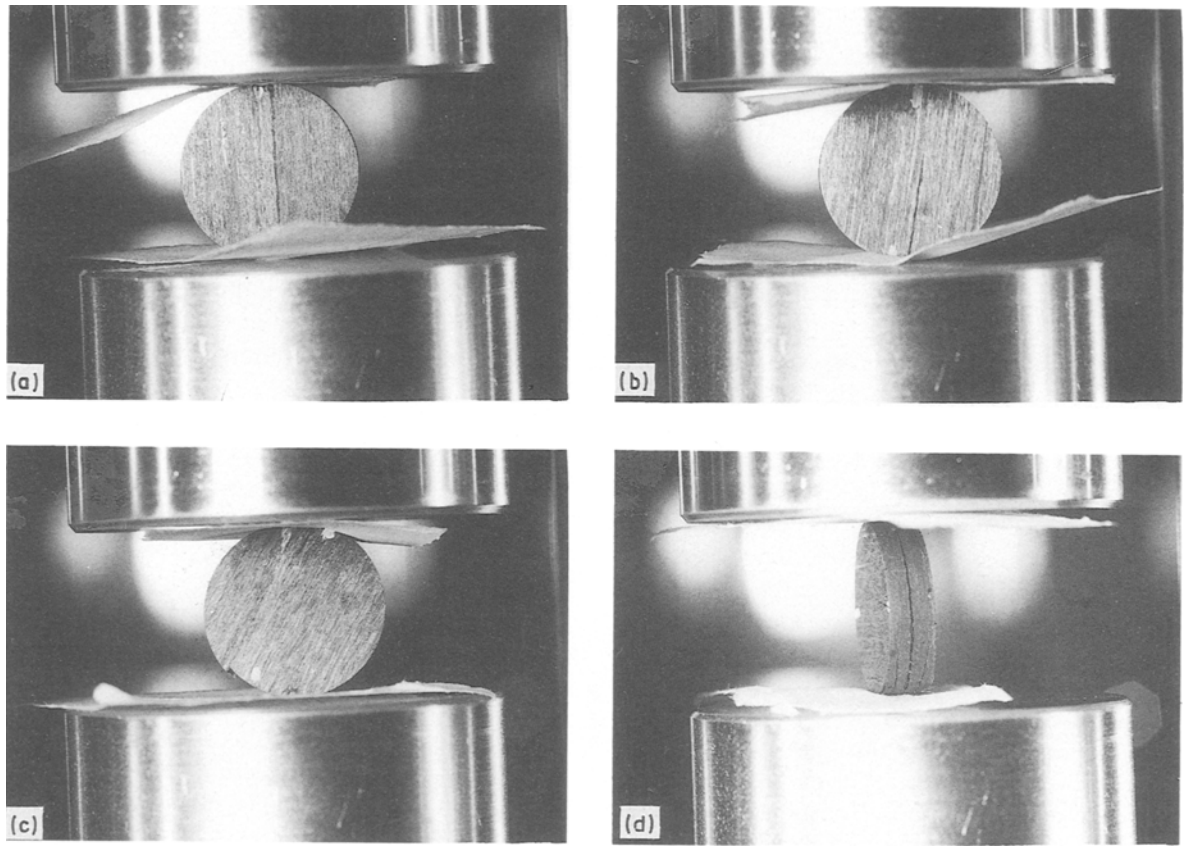

Figure 2 Cracks observed in the diametral compression tests. Angles between the fibre alignment and the loading axis are (a) 5°, (b) 10°, (c) 25°, and (d) 85°.

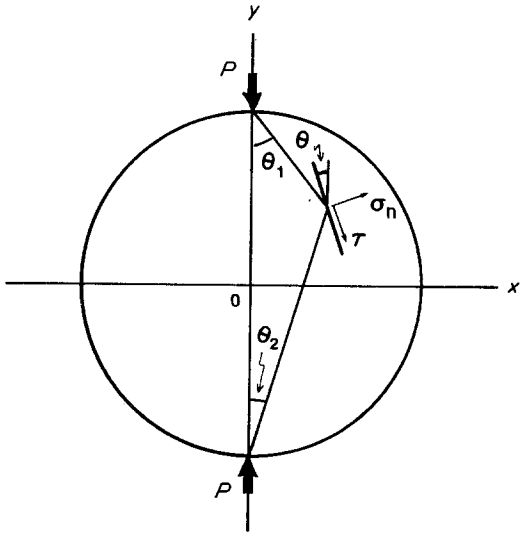

Figure 3 Stress under diametral compression. Stress components are shown for the inclined plane having angle, θ, from the loading axis.

through the loading point. This region starts from the opposite side of the loading point while the normal stress of the inclined plane at the loading point remains tensile.

Fig. 5 shows (a) the normal and (b) shear stress components in the inclined plane through the loading point plotted against the distance from the loading point. Calculation was done with $P = 1$, $t = 1$ and $R = 0.5$. When the angle, θ, is 0°, the tensile stress is a constant with $\tau = 0$ throughout this inclined plane. However, inclining the angle leads to a reduction in the normal tensile stress components and the appearance of the shear stress components. The stress components depend on the distance from the loading point, and the maximum tensile stress, σ_n^*, exists at the loading point. This value is obtained by letting $r_1 = 0$

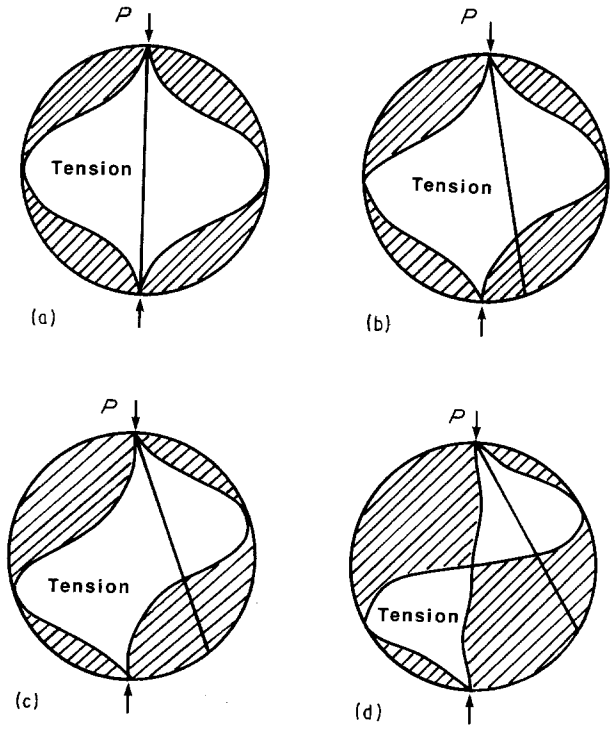

Figure 4 Normal stress components in the inclined plane with angle, θ, indicating compressive stress regions with hatched areas. (a) $\theta = 0°$, (b) $\theta = 10°$, (c) $\theta = 20°$, (d) $\theta = 30°$.

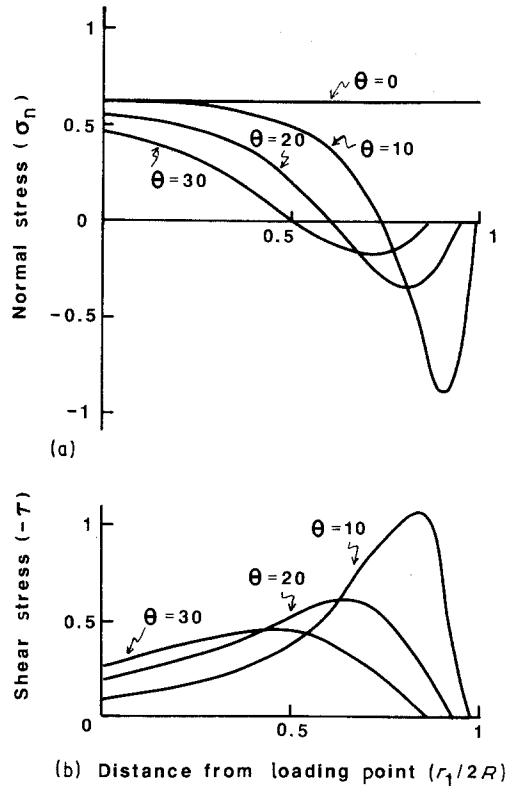

Figure 5 Stress component in the inclined plane through the loading point plotted against the distance from the loading point: (a) normal stress, (b) shear stress.

and $r_2 = 2R$ in Equation 1

$$\sigma_n^* = (P/\pi tR)\cos^2\theta \tag{3}$$

with the corresponding shear stress

$$\tau^* = (-P/\pi tR)\sin\theta\cos\theta \tag{4}$$

Although the stress states at the loading point seem to determine the fracture load on the basis of observation of the crack produced in the disc specimens, the complex biaxial stress states in the fibre-aligned plane fundamentally govern the fracture. Assuming that the pre-existing microcrack for producing the brittle fracture is located along the fibre axis, the crack extension under mixed-mode loading determines the fracture. Considering that the crack extension in the silicon carbide fibre-reinforced glass composite is limited to the direction along the fibre axis, the expressions for the mixed-mode fracture can then be simplified. The maximum normal stress criterion [1] is, for example, reduced to the simplified expression

$$K_{CR} = K_{IC} \tag{5}$$

Although the effect of the shear stress on the fracture of the composite under the diametral compression must be evaluated, the conventional expressions such as the non-coplanar energy release rate [3] and the minimum strain energy density [4] cannot be readily applied to the compressive stress region because they are reduced to the expression

$$K_{CR} = (K_I^2 + K_{II}^2)^{1/2} \tag{6}$$

This suggests the peculiar conclusion that the compression has the same effect on fracture as the tension, if we can define the negative K_I corresponding to it.

Moreover, even if the fracture does not occur in the compressive stress region, this expression results in a singularity of the criterion at $\sigma_n = 0$.

The expressions for the criterion applicable to the compression region should be chosen for the fracture analysis of the diametral compression tests. A practical expression for the mixed-mode fracture has been proposed under the K_I and K_{II} mode loading to be [9]

$$K_I/K_{IC} + (K_{II}/K_{IIC})^2 = 1 \quad (7)$$

This expression is applicable to fracture which includes the negative K_I region, provided the stable crack extension is negligible prior to catastrophic failure.

In order to evaluate the effects of shear stress on brittle fracture, we also have to consider the statistical aspect. The equivalent stress defined in the multiaxial stress state has been proposed [10] for explaining the statistical effects using the Weibull distribution function [11]. The equivalent stress, σ_e, for Equation 7 can be defined by

$$\sigma_e = \tfrac{1}{2}\{\sigma_n + [\sigma_n^2 + (2k\tau)^2]^{1/2}\} \quad (8)$$

where k is the ratio of K_{IC}/K_{IIC}. It should be noted that this equivalent stress is identical to the expression for the maximum normal stress criterion when $k = 0$.

The expression for the Weibull distribution function using the equivalent stress is given by

$$F = 1 - \exp\left[-\int_V (\sigma_e/\sigma_0)^m \, dV\right] \quad (9)$$

where F is the failure probability at volume, V, m is the Weibull modulus, and σ_0 is a scaling factor dependent on the material. In the diametral compression tests, it is noteworthy that σ_e as a function of the inclined angle, θ, is proportional to the applied load, P. We can thus define the normalized equivalent stress as $\sigma_e^* = \sigma_e/P$. Equation 9 then becomes

$$F = 1 - \exp\left[-(P/\sigma_0)^m \int_V \sigma_e^{*m} \, dV\right] \quad (10)$$

Letting the failure probability,F, be constant, we obtain the relation

$$P(\theta)^m \int_V \sigma_e^{*m} \, dV = \text{constant} \quad (11)$$

where $P(\theta)$ is the fracture load for the inclined angle, θ, at the fracture probability, F. Thus, $P(\theta)$ relative to $P(0)$ for $\theta = 0$ is expressed as

$$P(\theta)/P(0) = \left[\frac{\int_V \sigma_e^*(0)^m \, dV}{\int_V \sigma_e^*(\theta)^m \, dV}\right]^{1/m} \quad (12)$$

Fig. 6 shows the $P(\theta)/P(0)$ ratio, which is calculated from Equation 12 using the maximum normal stress criterion ($k = 0$) plotted against the inclined angle with a parameter of the Weibull modulus. The fracture load dependence on the inclined angle obtained from the diametral compression tests agrees with the calculated results for $m = 5$ to 10, which seems to be a reasonable value if we consider the scattering of the fracture load. This suggests that the maximum normal stress criterion governs the fracture.

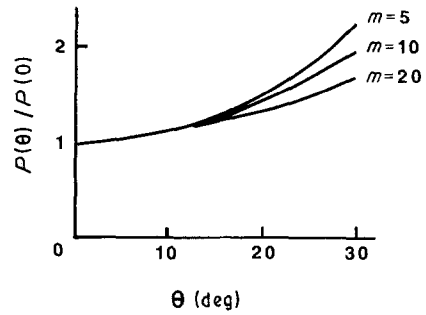

Figure 6 Computed fracture load dependence on the inclined angle. The fracture in the diametral compression tests is assumed to occur in the fibre-aligned plane being governed by the maximum normal stress criterion.

Nevertheless, consideration of shear stress on fracture results in an infinite shear component in the vicinity of the loading points (see Appendix). This would be a cause for the compressive local fracture under the loading points. In order to evaluate the effects of the shear stress on fracture, the calculation should be done under the assumption that the stress component near the loading points does not contribute to catastrophic failure. An analysis of the crushed zone size of the disc specimen suggests that the zone radius causing local fracture is approximately $R^* = 0.1R$.

Fig. 7 shows the calculated results of the $P(\theta)/P(0)$ ratio for the case of $R^* = 0.1R$ plotted against the

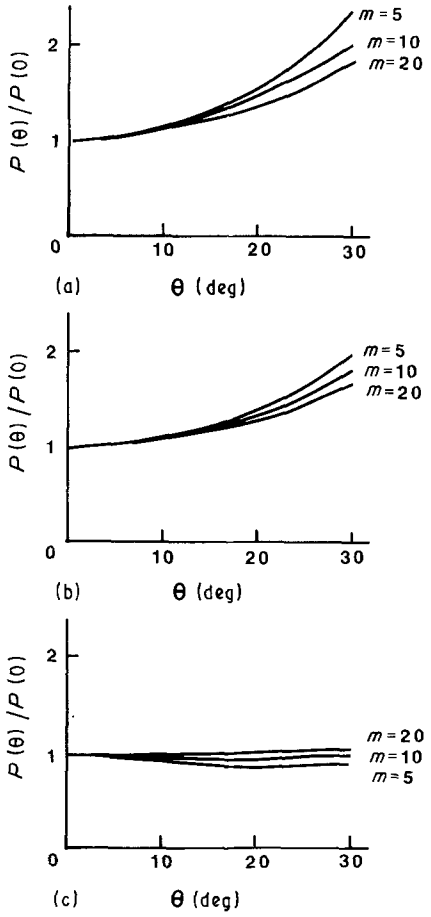

Figure 7 Computed fracture load dependence on the inclined angle for different k values with a damaged zone correction. Fracture in the diametral compression tests is assumed to occur in the fibre-aligned plane being governed by the mixed-mode fracture criterion. (a) $k = 0$, (b) $k = 0.2$, (c) $k = 0.5$.

inclined angle, θ, for different k values. This was done under the assumption that the stress components within the circle having the radius R^* under the loading point do not contribute to catastrophic failure. The increase in the fracture load with greater angle inclination is recognized for the cases of $k = 0$ and 0.2, while in the case of $k = 0.5$ the fracture load is almost completely independent of the inclined angle. The increase in the fracture load dependent on the inclined angle is greater when the ratio k, is smaller.

The considerable scattering of the data observed in the diametral compression tests suggests that the m value is relatively low: $m = 5$ to 10. The fracture load dependence on the inclined angle thus indicates that the k value is smaller than 0.2 even if we consider the effect of the local fracture under the loading point. The fact that the calculation for the case of the low k value where $m = 5$ to 10 agrees with the experimental results indicates that the effect of the shear stress on fracture is negligible.

4. Conclusion

Diametral compression tests for the unidimensionally aligned silicon carbide fibre-reinforced borosilicate glass were carried out, and the following conclusions were obtained.

1. When the angle between the loading axis and the alignment of the silicon carbide fibre is smaller than 30°, the crack extends along the fibre in the disc plane. This crack is initiated from the loading point and the fracture load increases with the increasing angle inclination.

2. From the stress analysis of the diametral compression tests, the fracture load seems to be governed by the normal tensile stress component applied to the plane along the fibre.

3. When the angle between the load axis and the silicon carbide fibre alignment exceeds 30°, the fracture occurs in the side of the disc at a nearly constant fracture load.

Acknowledgement

The author thanks Mitsuru Akama, Nippon Carbon Co., Ltd, for providing the specimens.

Appendix

Combining Equations 1 and 2, the shear stress, τ, in the inclined plane with angle, θ, is obtained as

$$\tau = P/\pi t \{[\cos\theta_1 \sin 2(\theta_1 - \theta)]/r_1 - [\cos\theta_2 \sin 2(\theta_2 + \theta)]/r_2\} \quad \text{(A1)}$$

where θ_1 and θ_2 are the coordinate angles shown in Fig. 3. Stress near the upper loading points can be given by letting $r_2 = 2R$ and $\theta_2 = 0$. Then, Equation A1 can be reduced to

$$\tau = P/\pi t\{[\cos\theta_1 \sin 2(\theta_1 - \theta)]/r_1 - [\sin(2\theta)]/2R\} \quad \text{(A2)}$$

This equation indicates that the maximum shear stress becomes infinite when r_1 approaches zero.

References

1. F. EROGEN and G. C. SIH, *J. Basic Engng* **85** (1963) 519.
2. D. C. PARIS and G. C. SIH, in ASTM STP 381 (American Society for Testing and Materials, Philadelphia, Pennsylvania, 1965) p. 30.
3. M. A. HUSSAIN, S. L. PU and J. UNDERWOOD, in ASTM STP. 560 (American Society for Testing and Materials, Philadelphia, Pennsylvania, 1974) p. 2.
4. G. C. SIH, *Int. J. Fract.* **10** (1974) 305.
5. W. F. BRUCE and E. G. BOMBOLAKIS, *J. Geophys. Res.* **68** (1963) 3709.
6. J. J. PETROVIC and M. G. MENDIRATTA, *J. Amer. Ceram. Soc.* **59** (1976) 164.
7. M. M. FROCHT, in "Photoelasticity", Vol. II (Wiley, New York, 1948) p. 121.
8. S. P. TIMOSHENKO and J. N. GOODIER, in "Theory of Elasticity", 3rd Edn (McGraw-Hill, New York, 1970) p. 19.
9. A. OKADA, *J. Mater. Sci.* **25** (1990) 1325.
10. S. B. BATDORF and H. L. HEINISCH Jr, *J. Amer. Ceram. Soc.* **61** (1978) 355.
11. W. WEIBULL, *J. Appl. Mech.* **18** (1951) 293.

Received 4 May
and accepted 29 September 1989